Journal of Lasers in Medical Sciences

J Lasers Med Sci 2024;15:e14

Original Article

http://journals.sbmu.ac.ir/jlms

doi 10.34172/jlms.2024.14

Evaluation of Near-Infrared Laser Effects on 143B Cells: A System Biology Approach

Mohammad Rostami Nejad[1], Masoumeh Farahani[2], Zahra Razzaghi[3], Babak Arjmand[4,5], Fatemeh Montazer[6], Fatemeh Bandarian[7], Farideh Razi[8], Mostafa Rezaei Tavirani[9*]

[1]Celiac Disease and Gluten Related Disorders Research Center, Research Institute for Gastroenterology and Liver Disease, Shahid Beheshti University of Medical Sciences, Tehran, Iran
[2]Skin Research Center, Shahid Beheshti University of Medical Sciences, Tehran, Iran
[3]Laser Application in Medical Sciences Research Center, Shahid Beheshti University of Medical Sciences, Tehran, Iran
[4]Cell Therapy and Regenerative Medicine Research Center, Endocrinology and Metabolism Molecular-Cellular Sciences Institute, Tehran University of Medical Sciences, Tehran, Iran
[5]Iranian Cancer Control Center (MACSA), Tehran, Iran
[6]Department of Pathology, Firoozabadi Hospital, School of Medicine, Iran University of Medical Sciences, Tehran, Iran
[7]Endocrinology and Metabolism Research Center, Endocrinology and Metabolism Clinical Sciences Institute, Tehran University of Medical Sciences, Tehran, Iran
[8]Diabetes Research Center, Endocrinology and Metabolism Clinical Sciences Institute, Tehran University of Medical Sciences, Tehran, Iran
[9]Proteomics Research Center, Faculty of Paramedical Sciences, Shahid Beheshti University of Medical Sciences, Tehran, Iran

***Correspondence to**
Mostafa Rezaei Tavirani,
Email: tavirany@yahoo.com

Received: January 28, 2024
Accepted: February 19, 2024
ePublished: June 2, 2024

Abstract

Introduction: Photothermal therapy (PTT) by using a near-infrared (NIR) laser, as a successful treatment of cancer, has attracted extensive attention of researchers. Its advantages as a noninvasive and suitable method have been confirmed. Discovery of the NIR laser molecular mechanism at the cellular level via system biology assessment to identify the crucial targeted genes is the aim of this study.

Methods: RNA-seq series of six samples were retrieved from Gene Expression Omnibus (GEO) and pre-evaluated by the GEO2R program for more analysis. The significant differentially expressed genes (DEGs) were determined and studied via gene expression analysis, protein-protein interaction (PPI) network assessment, action map evaluation, and gene ontology enrichment.

Results: HSPA5, DDIT3, TRIB3, PTGS2, HMOX1, ASNS, GDF15, SLC7A11, and SQSTM1 were identified as central genes. Comparing the central genes and the determined crucial genes via gene expression analysis, actin map results, and gene ontology enrichment led to the introduction of HSPA5, DDIT3, PTGS2, HMOX1, and GDF15 as critical genes in response to the NIR laser.

Conclusion: The results indicated that the principle biological process "Endoplasmic reticulum unfolded protein response" and HSPA5, DDIT3, PTGS2, HMOX1, and GDF15 are the crucial targets of the NIR laser. The results also showed that the NIR laser induces stress conditions in the irradiated cells.

Keywords: Near infrared; Osteosarcoma; Treatment; Network analysis; Gene ontology.

Introduction

As external stimuli, light, ultrasound, and magnetic field are able to activate cancerous targets in vivo. The NIR laser can be applied as an efficient stimulus to mark the cancer thermo-chemotherapy targets.[1] NIR as a tool of photothermal therapy (PTT) has attracted extensive attention as a successful treatment of cancer. It has appeared as a noninvasive and effective method.[2] Development of PTT is associated with applying suitable particles that are able to penetrate deeply into cancer tissue and using the NIR laser to raise the temperature in targeted tissue.[3] In this regard, researchers try to introduce new photodynamic therapy sensitizers to promote the usage of NIR as a beneficial method against cancer.[4]

Both genomics and bioinformatics are applied to explore the molecular mechanism of many therapeutic methods. There are documents about the genomic study of NIR application in medicine.[5,6] Bioinformatics as a well-known technique is used widely to discover the molecular mechanism of diseases and methods in medicine.[7] It has been established that the gene expression profile study is a successful approach to exploring the details of the molecular

Please cite this article as follows: Rostami Nejad M, Farahani M, Razzagh Z, Arjmand B, Montazer F, Bandarian F, et al. Evaluation of near-infrared laser effects on 143B cells: a system biology approach. *J Lasers Med Sci.* 2024;15:e14. doi:10.34172/jlms.2024.14.

event in diseases, especially cancers.[8,9] Interesting data have been produced about the effect of radiation on the cells and body via genomic studies. There are many published data about gene expression alteration following exposure to IR radiation.[10,11] The close relationship between genomics and bioinformatics has accelerated the simplification of complex results of genomics.[12]

Protein-protein interaction (PPI) network analysis is a tool to study a large set of genes to find the crucial individuals. In this method genes make connections with the neighbor(s) to form an interactome based on their specific centrality properties. The central genes, hubs, and bottlenecks are critical elements of a PPI network. The central nodes control other nodes of the network and also the related critical functions.[13,14] PPI network analysis is applied widely to study biological systems after exposure to radiation.[15,16] Gene ontology assessment is another approach that is applied broadly to identify the altered biological processes and biochemical pathways.[17] In the present study, gene expression data related to the effect of the NIR laser on osteosarcoma cells (143B cell line) were retrieved from the GEO database, and they were evaluated via PPI network analysis and gene ontology assessment to explore more details of related cellular molecular events.

Methods

Data Collection

Information about osteosarcoma cells (143B cell line) which were treated with near-infrared (NIR) was extracted from GSE11393 (https://www.ncbi.nlm.nih.gov/geo/geo2r/?acc=GSE211393) that was recorded in the GEO database. The cells received TPBC-PEG (tetraphenyl bacteriochlorin-mono-functional polyethylene glycol) as a photosensitizer and were exposed to a laser for 4 minutes (160 mV, 735 nm), followed by a 24-hour culture. RNA-seq data of the cells (GSM6468381-3) were compared with controls (GSM6468378-80). The significant differentially expressed genes (DEGs) were determined by using the FEO2R program.

Pre-evaluation Analysis

To explore the distribution pattern of significant up- and downregulated DEGs, we provided a volcano plot. The separation of the treated 143B cells from the controls was assessed via UMAP analysis. The numbers of DEGs and Significant DEGs were visualized via a Venn diagram. The relationship between the normalized average of gene expression values and the related dispersion parameters was assessed via the mean – variance trend.

Gene Expression Analysis

Gene expression change is a critical property of the studied biological samples. In the present study, about 10% of the top up and down-regulated DEGs were selected for more analysis.

Network Analysis

The significant DEGs were assessed via PPI network analysis by using the STRING database and Cytoscape software v 3.7.2. The main connected component of the PPI network was analyzed via the "Network analyzer" application of Cytoscape to find the central nodes. The top 10% of nodes based on degree value and betweenness centrality were identified as hubs and bottlenecks, respectively. The common hubs and bottlenecks were introduced as hub-bottlenecks. Expression, activation, and inhibition relationships between significant DEGs were assessed via CluePedia. The significant DEGs were enriched via CluGO to find associated biological processes.

Statistical Analysis

Significant DEGs were identified based on the adjusted p-value of less than 0.05. Significant DEGs with $1 \leq \text{LogFC} \leq (-1)$ were considered for more analysis. The PPI network was constructed by considering confidence score = 0.2. Biological processes were determined by considering term p-value, term p-value corrected with Bonferroni step-down, group p-value, and group p-value corrected with Bonferroni step-down less than 0.01.

Results

The distribution of up- and downregulated DEGs is visualized in Figure 1. There are many significant DEGs that discriminate the 143B cells treated with the NIR laser from the controls. UMAP analysis (Figure 2) revealed that the treated cells and controls are differentiated completely. As shown in Figure 3, there are 4714 significant DEGs relative to the 17 333 total dysregulated genes. Since a 2-fold change is a suitable criterion to select the significant DEGs,[18] the number of the significant DEGs was limited by the application of this parameter. The normalized average of the gene expression values and the related dispersion parameters (Figure 4) indicates that the analysis is acceptable and the statistical parameters are defined properly.

The three most downregulated and 16 most upregulated genes were selected among the significant DEGs. The gene expression change values of the most dysregulated genes are shown in Figure 5. 170 significant DEGs were included in the STRING database to form the PPI network. Among the queried DEGs, 143 genes (including 7 isolated DEGs and a main connected component of 136 nodes) were recognized. The main connected component of the PPI network is presented in Figure 6. Fourteen hubs and 14 bottlenecks were introduced. Finally, nine hub-bottleneck genes including HSPA5, DDIT3, TRIB3, PTGS2, HMOX1, ASNS, GDF15, SLC7A11, and SQSTM1were introduced as central DEGs (see Table 1).

The results of the action map analysis are shown in Figure 7. As it is depicted in Figure 7, seven subnetworks

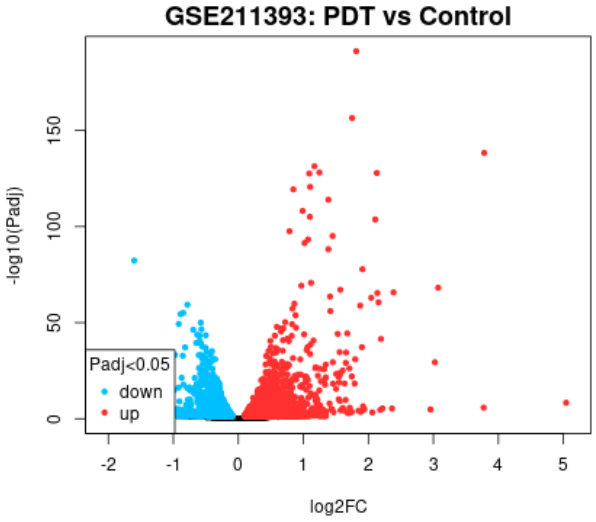

Figure 1. Volcano Plot of Cell Response to the NIR Laser

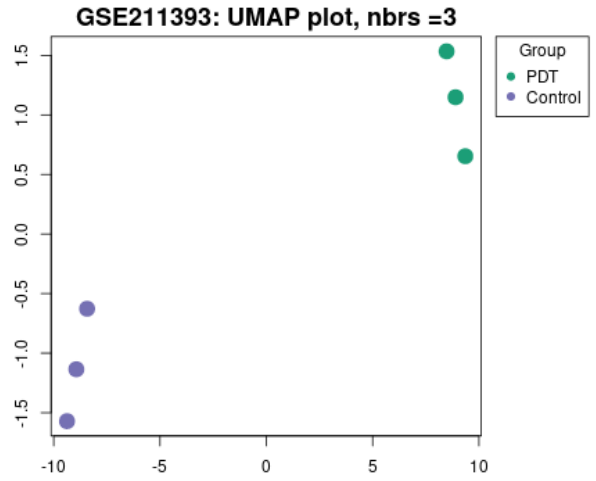

Figure 2. UMAP of the Gene Expression Analysis of the Treated Cells with the NIR Laser Versus the Control

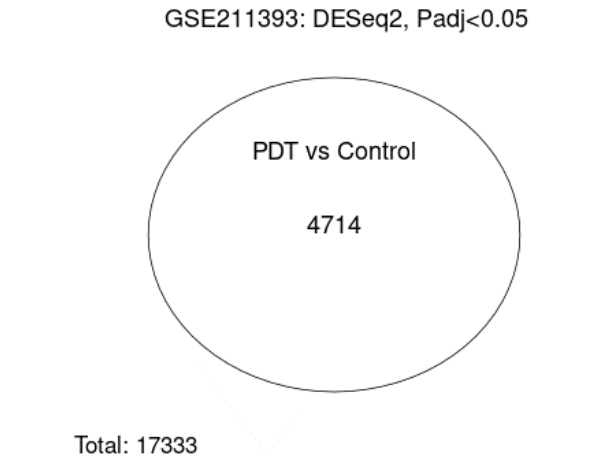

Figure 3. Venn Diagram of the Gene Expression Analysis of the Treated Cells with the NIR Laser Versus the Control

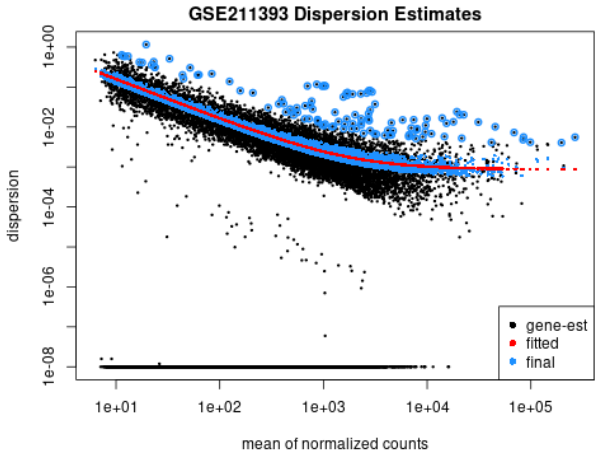

Figure 4. Mean – Variance Trend of the Gene Expression Analysis of the Treated Cells with the NIR Laser Versus the Control

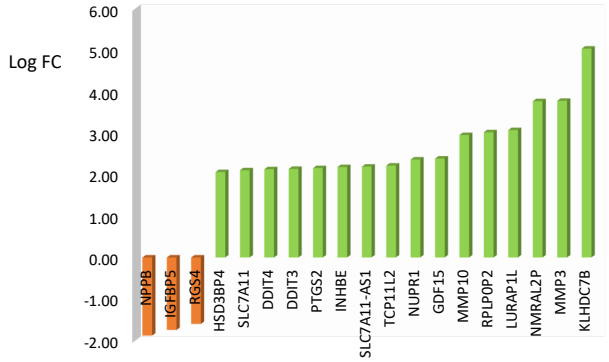

Figure 5. Top Up- and Downregulated Genes Related to the Gene Expression Analysis of the Treated Cells with the NIR Laser Versus the Control

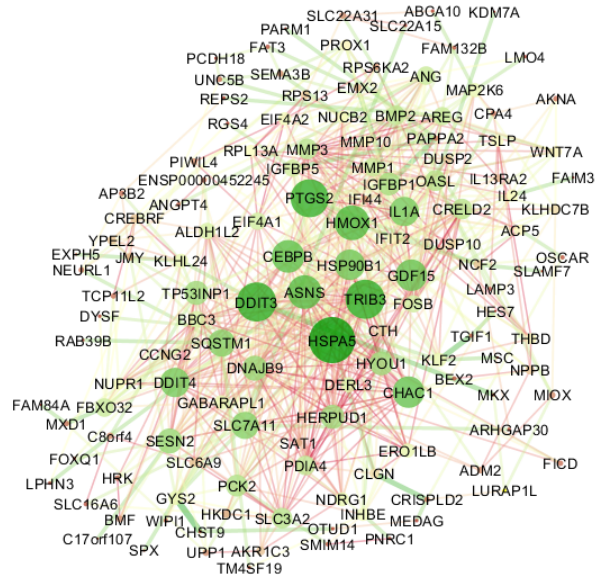

Figure 6. Main Connected Component of the PPI Network. Red to green and small to large refer to the increment of degree values and betweenness centralities

are formed. The studied nodes are connected mostly to others via activation action. The associated biological to significant DEGs are shown in Figure 8. As it is presented in Figure 8, 36 biological processes are grouped into 13

Table 1. List of the hub-bottleneck DEGs of the main connected component

Display Name	Description	Degree	Betweenness Centrality	LogFC
HSPA5	heat shock protein family A (Hsp70) member 5	40	0.080	2.04
DDIT3	DNA damage inducible transcript 3	35	0.070	2.14
TRIB3	tribbles pseudokinase 3	35	0.057	1.57
PTGS2	prostaglandin-endoperoxide synthase 2	34	0.072	2.16
HMOX1	heme oxygenase 1	31	0.055	1.04
ASNS	Asparagine synthetase (glutamine-hydrolyzing)	30	0.045	1.45
GDF15	growth differentiation factor 15	28	0.051	2.39
SLC7A11	SLC7A11 antisense RNA 1	24	0.050	2.19
SQSTM1	sequestosome 1	24	0.059	1.02

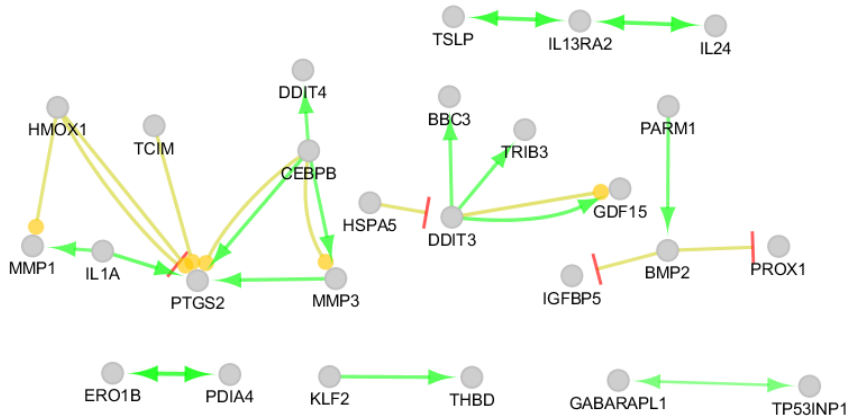

Figure 7. Action Map Related to the Gene Expression Analysis of the Treated Cells With the NIR Laser Versus the Control. Green and yellow refer to activation and expression

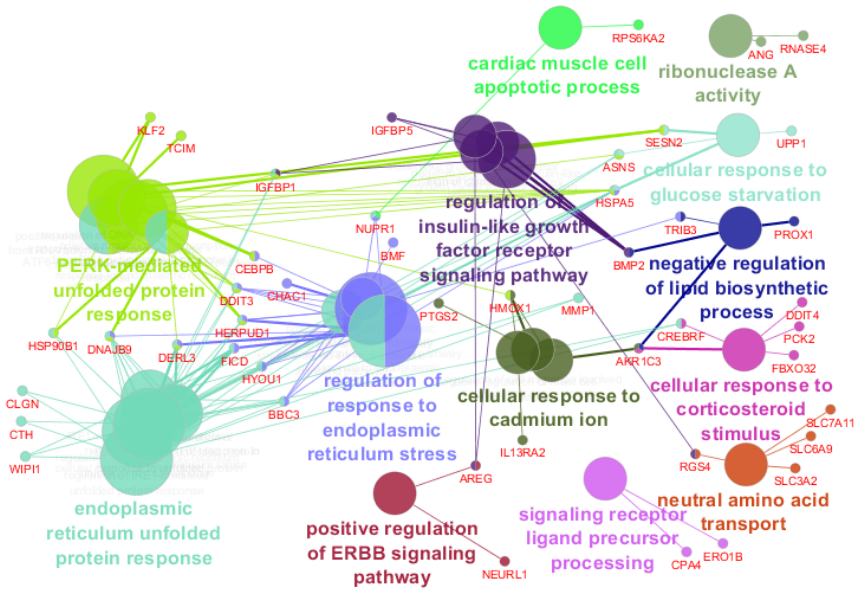

Figure 8. Biological Processes and Associated Significant DEGs (the red labeled nodes)

clusters. Eight clusters have a single member, while the largest cluster include 11 biological processes. The two largest clusters and the associated DEGs are shown in Figure 9.

Discussion

The effect of IR radiation on the gene expression of osteosarcoma cells (143B cell line) has attracted researchers' attention. Apoptosis extracellular matrix, stress signaling, and calcium homeostasis are introduced as the targets of IR radiation.[19] Pre-evaluation of the data revealed that the NIR laser has changed the gene expression of the treated 143B cells effectively. 4714 significant DEGs (a large set of genes) were introduced

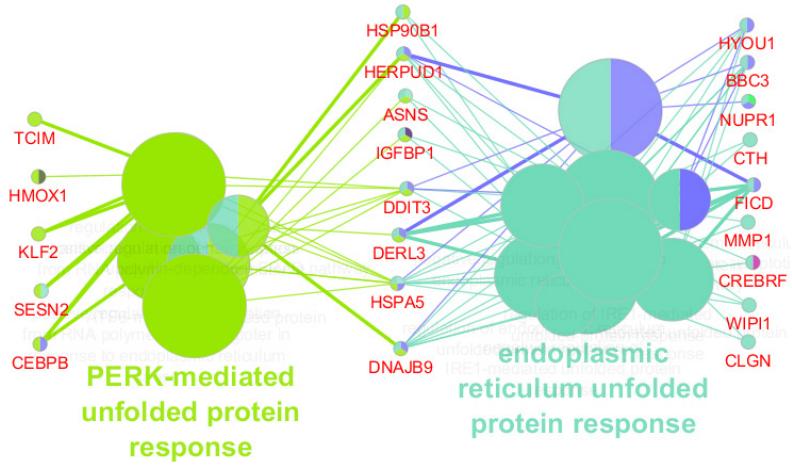

Figure 9. The Two Largest Groups of Biological Processes and Associated Significant DEGs (the red labeled nodes)

as a response to the NIR laser. Four steps of analyses including gene expression, PPI network, action map, and gene ontology evaluations were planned to explore the crucial genes among 4714 significant DEGs.

Gene expression analysis is a useful method for assessing biological events.[20] In the first step, a set of genes including NPPB, IGFBP5, RGS4, HSD3BP4, SLC7A11, DDIT4, DDIT3, PTGS2, INHBE, SLC7A11-AS1, TCP11L2, NUPR1, GDF15, MMP10, RPLP0P2, LURAP1L, NMRAL2P, MMP3, and KLHDC7B was identified as the top dysregulated genes. Since the central nodes of a PPI network are considered as important individuals that play critical roles in functions of the studied system,[21] in the second step of the study, the central nodes of the PPI network were considered for more investigation. An action map includes seven subnetworks: three paired nodes, two triples, a pentad, and a component of eight nodes. An action map as an efficient method is applied to understand the molecular mechanism of diseases.[22] In the third step of the analysis, the subnetworks that had common genes with gene expression analysis or PPI network results were selected for more analysis. Based on this assessment, the three paired subnetworks and the triples including TSLP, IL13RA2, and IL24 that are shown in Figure 7 were ignored for further analysis. The remained subnetworks include 17 DEGs (see Figure 7). Finally, 22 genes were determined as the important individual from gene ontology assessment. Gene ontology is used as a tool to screen genomics data by researchers.[22]

The assessment indicated that the SQSTM1 central node was not included in the other three gene sets. Therefore, SQSTM1 was deleted from the critical genes. A similar investigation showed that TRIB3, ASNS, and SLC7A11 were common with only one gene set, and they were ignored for more evaluation. HSPA5, DDIT3, PTGS2, HMOX1, and GDF15 remained as the central genes that were included in at least 2 gene sets. These five central genes were pointed out as the critical genes which were targeted by the NIR laser.

Heat shock protein family A (Hsp70) member 5 (HSPA5) is unreasonably expressed in various tumors and closely accompanied by the development and prognosis of cancer.[23] As it is shown in Figure 7, HSPA5 downregulates DDIT3 (the second critical gene). DNA damage inducible transcript (DDIT3) is a pro-apoptotic transcription factor that is associated with endoplasmic reticulum-stress response.[24] It is reported that HSPA5 is accompanied by protein folding in the endoplasmic reticulum cellular compartment.[25] The relationship between DDIT3 and Growth differentiation factor 15 (GDF15) is shown in Figure 7. DDIT3 activates and upregulates GDF15. Based on evidence, GDF15 as a cytokine has a significant effect on systemic energy metabolism. An investigation indicates that GDF15 expression and secretion are often linked to mitochondrial stress. Various stress conditions such as acute myocardial infarction and intense exercise induce GDF15 expression.[26]. As it is represented in Figure 7, the pentad subnetwork is a crucial component which includes three critical central genes. This component also contains TRIB3 (the central node) which is introduced in Table 1. Research showed that TRIB3 changes endoplasmic reticulum stress-induced β-cell apoptosis.[27]

A close relationship between prostaglandin-endoperoxide synthase 2 (PTGS2) and heme oxygenase 1 (HMOX1) is seen in Figure 7. The relationship between PTGS2 upregulation and increased radio-resistance in glioma cells has been evaluated previously.[28] The positive effect of HMOX1 upregulation as an adaptive mechanism on the protection of cells from oxidative damage during stress is a well-known role of HMOX1.[29] The crucial roles of the critical central genes in "endoplasmic reticulum unfolded protein response" and "PERK-mediated unfolded protein response" biological processes are depicted in Figure 9. "Endoplasmic reticulum unfolded protein response" as the main group of biological process includes 11 biological processes.

Conclusion

In conclusion, the NIR laser induces considerable alterations in the gene expression profiles of the treated osteosarcoma cells. HSPA5, DDIT3, PTGS2, HMOX1, and GDF15 were introduced as five critical targets of the NIR laser in osteosarcoma cells (143B cell line). The results showed that "endoplasmic reticulum unfolded protein response" is the principal biological process group which is affected by the NIR laser. It can be concluded that the NIR laser like other types of radiation induces stress conditions in the irradiated cells. It can be suggested that the efficiency and possible side effects of NIR laser application to treat cancer be compared with the other radiation methods.

Acknowledgments

This project is supported by Shahid Beheshti University of Medical Sciences.

Authors' Contribution

Conceptualization: Mostafa Rezaei Tavirani, Farideh Razi, Fatemeh Montazer.
Data curation: Zahra Razzaghi, Fatemeh Bandarian.
Formal analysis: Zahra Razzaghi.
Funding acquisition: Mostafa Rezaei Tavirani.
Investigation: Mohammad Rostami Nejad, Fatemeh Montazer.
Methodology: Masoumeh Farahani.
Project administration: Mohammad Rostami Nejad, Fatemeh Bandarian, Babak Arjmand.
Resources: Masoumeh Farahani.
Software: Masoumeh Farahani.
Supervision: Mostafa Rezaei Tavirani, Babak Arjmand.
Validation: Farideh Razi, Fatemeh Montazer.
Visualization: Zahra Razzaghi.
Writing–original draft: Mostafa Rezaei Tavirani, Farideh Razi, Babak Arjmand.
Writing–review & editing: Mostafa Rezaei Tavirani, Mohammad Rostami Nejad, Fatemeh Bandarian.

Competing Interests

There is no conflict of interest.

Ethical Approval

Not applicable.

Funding

This work was financially supported by Shahid Beheshti University of Medical Sciences, Tehran, Iran.

References

1. Zhang Z, Wang J, Nie X, Wen T, Ji Y, Wu X, et al. Near infrared laser-induced targeted cancer therapy using thermoresponsive polymer encapsulated gold nanorods. J Am Chem Soc. 2014;136(20):7317-26. doi: 10.1021/ja412735p.
2. Wu X, Suo Y, Shi H, Liu R, Wu F, Wang T, et al. Deep-tissue photothermal therapy using laser illumination at NIR-IIa window. Nanomicro Lett. 2020;12(1):38. doi: 10.1007/s40820-020-0378-6.
3. Liu FH, Cong Y, Qi GB, Ji L, Qiao ZY, Wang H. Near-infrared laser-driven in situ self-assembly as a general strategy for deep tumor therapy. Nano Lett. 2018;18(10):6577-84. doi: 10.1021/acs.nanolett.8b03174.
4. Starkey JR, Rebane AK, Drobizhev MA, Meng F, Gong A, Elliott A, et al. New two-photon activated photodynamic therapy sensitizers induce xenograft tumor regressions after near-IR laser treatment through the body of the host mouse. Clin Cancer Res. 2008;14(20):6564-73. doi: 10.1158/1078-0432.ccr-07-4162.
5. Peng H, Le C, Wu J, Li XF, Zhang H, Le XC. A genome-editing nanomachine constructed with a clustered regularly interspaced short palindromic repeats system and activated by near-infrared illumination. ACS Nano. 2020;14(3):2817-26. doi: 10.1021/acsnano.9b05276.
6. Sasaki Y, Oshikawa M, Bharmoria P, Kouno H, Hayashi-Takagi A, Sato M, et al. Near-infrared optogenetic genome engineering based on photon-upconversion hydrogels. Angew Chem Int Ed Engl. 2019;58(49):17827-33. doi: 10.1002/anie.201911025.
7. Han Z, Zhang Y, Wang P, Tang Q, Zhang K. Is acupuncture effective in the treatment of COVID-19 related symptoms? Based on bioinformatics/network topology strategy. Brief Bioinform. 2021;22(5):bbab110. doi: 10.1093/bib/bbab110.
8. Poulin JF, Gaertner Z, Moreno-Ramos OA, Awatramani R. Classification of midbrain dopamine neurons using single-cell gene expression profiling approaches. Trends Neurosci. 2020;43(3):155-69. doi: 10.1016/j.tins.2020.01.004.
9. Brady L, Kriner M, Coleman I, Morrissey C, Roudier M, True LD, et al. Inter- and intra-tumor heterogeneity of metastatic prostate cancer determined by digital spatial gene expression profiling. Nat Commun. 2021;12(1):1426. doi: 10.1038/s41467-021-21615-4.
10. Labbé M, Hoey C, Ray J, Potiron V, Supiot S, Liu SK, et al. microRNAs identified in prostate cancer: correlative studies on response to ionizing radiation. Mol Cancer. 2020;19(1):63. doi: 10.1186/s12943-020-01186-6.
11. Schieke SM, Schroeder P, Krutmann J. Cutaneous effects of infrared radiation: from clinical observations to molecular response mechanisms. Photodermatol Photoimmunol Photomed. 2003;19(5):228-34. doi: 10.1034/j.1600-0781.2003.00054.x.
12. Birdsell JA. Integrating genomics, bioinformatics, and classical genetics to study the effects of recombination on genome evolution. Mol Biol Evol. 2002;19(7):1181-97. doi: 10.1093/oxfordjournals.molbev.a004176.
13. Zito A, Lualdi M, Granata P, Cocciadiferro D, Novelli A, Alberio T, et al. Gene set enrichment analysis of interaction networks weighted by node centrality. Front Genet. 2021;12:577623. doi: 10.3389/fgene.2021.577623.
14. Rasti S, Vogiatzis C. Novel centrality metrics for studying essentiality in protein-protein interaction networks based on group structures. Networks. 2022;80(1):3-50. doi: 10.1002/net.22071.
15. Sekaran TS, Kedilaya VR, Kumari SN, Shetty P, Gollapalli P. Exploring the differentially expressed genes in human lymphocytes upon response to ionizing radiation: a network biology approach. Radiat Oncol J. 2021;39(1):48-60. doi: 10.3857/roj.2021.00045.
16. Arjmand B, Rezaei-Tavirani M, Hamzeloo-Moghadam M, Razzaghi Z, Khodadoost M, Okhovatian F, et al. Hypofractionated radiation versus conventional fractionated radiation: a network analysis. J Lasers Med Sci. 2022;13:e39. doi: 10.34172/jlms.2022.39.
17. Zhang YH, Zeng T, Chen L, Huang T, Cai YD. Determining protein-protein functional associations by functional rules based on gene ontology and KEGG pathway. Biochim Biophys Acta Proteins Proteom. 2021;1869(6):140621. doi: 10.1016/j.bbapap.2021.140621.
18. Dalman MR, Deeter A, Nimishakavi G, Duan ZH. Fold change and p-value cutoffs significantly alter microarray

interpretations. BMC Bioinformatics. 2012;13(Suppl 2):S11. doi: 10.1186/1471-2105-13-s2-s11.
19. Calles C, Schneider M, Macaluso F, Benesova T, Krutmann J, Schroeder P. Infrared A radiation influences the skin fibroblast transcriptome: mechanisms and consequences. J Invest Dermatol. 2010;130(6):1524-36. doi: 10.1038/jid.2010.9.
20. Costa-Silva J, Domingues DS, Menotti D, Hungria M, Lopes FM. Temporal progress of gene expression analysis with RNA-Seq data: a review on the relationship between computational methods. Comput Struct Biotechnol J. 2023;21:86-98. doi: 10.1016/j.csbj.2022.11.051.
21. Altaf-Ul-Amin M, Wijaya SH, Chandra DF, Kanaya S. Centrality values of yeast proteins in a PPI network are related to their essentiality and functions. J Comput Aided Chem. 2017;18:94-109.
22. Zamanian-Azodi M, Arjmand B, Razzaghi M, Rezaei Tavirani M, Ahmadzadeh A, Rostaminejad M. Platelet and haemostasis are the main targets in severe cases of COVID-19 infection; a system biology study. Arch Acad Emerg Med. 2021;9(1):e27. doi: 10.22037/aaem.v9i1.1108.
23. Wang Q, Ke S, Liu Z, Shao H, He M, Guo J. HSPA5 promotes the proliferation, metastasis and regulates ferroptosis of bladder cancer. Int J Mol Sci. 2023;24(6):5144. doi: 10.3390/ijms24065144.
24. Block I, Müller C, Sdogati D, Pedersen H, List M, Jaskot AM, et al. CFP suppresses breast cancer cell growth by TES-mediated upregulation of the transcription factor DDIT3. Oncogene. 2019;38(23):4560-73. doi: 10.1038/s41388-019-0739-0.
25. Wang J, Lee J, Liem D, Ping P. HSPA5 gene encoding Hsp70 chaperone BiP in the endoplasmic reticulum. Gene. 2017;618:14-23. doi: 10.1016/j.gene.2017.03.005.
26. Johann K, Kleinert M, Klaus S. The role of GDF15 as a myomitokine. Cells. 2021;10(11). doi: 10.3390/cells10112990.
27. Fang N, Zhang W, Xu S, Lin H, Wang Z, Liu H, et al. TRIB3 alters endoplasmic reticulum stress-induced β-cell apoptosis via the NF-κB pathway. Metabolism. 2014;63(6):822-30. doi: 10.1016/j.metabol.2014.03.003.
28. Lin S, Shen Z, Yang Y, Qiu Y, Wang Y, Wang X. Expression profiles of radio-resistant genes in colorectal cancer cells. Radiat Med Prot. 2021;2(2):48-54. doi: 10.1016/j.radmp.2021.04.006.
29. Poss KD, Tonegawa S. Reduced stress defense in heme oxygenase 1-deficient cells. Proc Natl Acad Sci U S A. 1997;94(20):10925-30. doi: 10.1073/pnas.94.20.10925.